

Sahlu, S. & Abebe, A. (2026). Diffusive dark fluids with Planck-2018 and DESI BAO DR2 measurements. In Abebe, A. & Paliathanasis, A. (eds), *Proceedings of the South African Gravity Society Conference 2025 (SAGS2025)*. Potchefstroom: Axiom Academic Publishers, pp. 37 - 48.

CHAPTER 4

Diffusive dark fluids with Planck-2018 and DESI BAO DR2 measurements

Shambel Sahlu and Amare Abebe

Abstract

In this paper, we constrain the diffusive dark fluid cosmological model, wherein energy is transferred between the two dark components through a diffusion process. We extended the work in Ref. [1] by employing Cosmic Microwave Background (CMB) data from the Planck 2018 measurements in combination with Baryon Acoustic Oscillation (BAO) data from the Dark Energy Spectroscopic Instrument (DESI) DR2 (2024). From the results, we found that the discrepancies in H_0 measurements are 1.90σ and 1.72σ between the Planck 2018 value $(H_0 = 67.4 \pm 0.5\,\mathrm{km, s^{-1}, Mpc^{-1}})$ and our diffusive model values, $H_0 = 67.27^{+0.54}_{-0.55}$, and $68.35^{+0.31}_{-0.29}$, respectively. We also observe that the effects of the interaction on cosmic evolution and structure formation; we emphasize this by computing the scale-dependent density contrast and the matter power spectrum, compared with the ΛCDM model.

Keywords: Interacting dark sector; diffusion; Planck 2018; DESI BAO; Hubble tension

Diffusive dark fluids with Planck-2018 and DESI BAO DR2 Measurements

Shambel Sahlu*[1,2] and Amare Abebe†[1,2]

[1]Centre for Space Research, North-West University, Potchefstroom 2520, South Africa
[2]National Institute for Theoretical and Computational Sciences (NITheCS), South Africa

Abstract

In this paper, we constrain the diffusive dark fluid cosmological model, wherein energy is transferred between the two dark components through a diffusion process. We extended the work in Ref. [1] by employing Cosmic Microwave Background (CMB) data from the Planck 2018 measurements in combination with Baryon Acoustic Oscillation (BAO) data from the Dark Energy Spectroscopic Instrument (DESI) DR2 (2024). From the results, we found that the discrepancies in H_0 measurements are 1.90σ and 1.72σ between the Planck 2018 value ($H_0 = 67.4 \pm 0.5\ \mathrm{km\,s^{-1}\,Mpc^{-1}}$) and our diffusive model values, $H_0 = 67.27^{+0.54}_{-0.55}$, and $68.35^{+0.31}_{-0.29}$, respectively. We also observe that the effects of the interaction on cosmic evolution and structure formation; we emphasize this by computing the scale-dependent density contrast and the matter power spectrum, compared with the ΛCDM model.

1 Introduction

The standard model of cosmology, the so-called ΛCDM model, explains a wide range of cosmological phenomena successfully; refer to the references [2–7]. However, modern cosmology increasingly faces significant challenges, as different cosmological measurements have shown that the universe has been experiencing accelerated expansion due to the exotic fluid known as dark energy [2, 8], which accounts for $\sim 70\%$ of the universe. Another mysterious component of the universe, referred to as dark matter or missing matter, accounts for $\sim 25\%$ of the universe, posing a challenge for modern physics. These major dark components of the universe represent puzzles in physics [9, 10]. The energy density ratio of dark matter to dark energy (ρ_{dm}/ρ_{de}, where ρ_{dm} is the energy density of dark matter and ρ_{de} represents the density of dark energy) can decline more slowly than a^{-3} (where a is the scale factor), indicating that there is an energy exchange between dark matter and dark energy, as supported by the interacting dark sector models. In such models, the interaction term Q accounts for the exchange of energy between dark matter and dark energy without non-gravitational interactions.

*shambel.sahlu@nithecs.ac.za
†amare.abebe@nithecs.ac.za

The interaction model has been proposed to address different cosmological probes [11–14]. For instance, a broad discussion of the influence of the interaction between early dark energy and dark matter, and its effects on structure growth and the CMB, is presented in the Refs. [15, 16]. In these references, the parameters of the early dark energy model and the coupling between the dark sectors have been constrained using various observational data. The work presented in [17] also emphasized the role of CMB probes in interacting dark energy models, utilizing data from the Planck satellite, the Atacama Cosmology Telescope, and WMAP (9-year data). According to their results, the values of H_0 are modified due to the transfer of energy from dark matter to dark energy. The growth factor and weak lensing signals for a new class of interacting dark energy models are discussed in Ref. [18]. Furthermore, the growth structure of the universe has been explored in [19], where the influence of non-vanishing dark energy perturbations on the evolution of dark matter perturbations has been analyzed in detail. In another study, [20] conducted detailed N-body simulations to investigate dark energy models, focusing on the formation of cosmic structures and the properties of dark matter halos. Due to the decay of energy from matter to dark energy, structure formation is slowed down, which leads to inconsistencies with observed structure formation. Consequently, the interacting model can be ruled out based on non-linear structure formation, as the interaction term Q is highly sensitive. Similar discrepancies have been reported by [21], who concluded that the universality of the halo mass function is violated in cosmological models featuring direct interactions between dark energy and cold dark matter. Interacting dark energy models are the most promising models for solving the cosmological tensions. In the work [22], an evolving dark energy field with an appropriate non-gravitational interaction with matter is introduced to solve the coincidence problem, since the ratio of matter to dark energy density is expected to decrease rapidly proportional to the scale factor as the universe expands. The potential of the interacting dark energy model to solve the Hubble tension H_0 in km/s/Mpc is reported by [22, 23], which is one of the current challenges in the measurements between the direct and indirect measurements.

In this manuscript, we focus on an interaction model in which energy is transferred between dark matter and dark energy, or vice versa, through a diffusion mechanism [24–26], as broadly discussed in the work [1] using late-time measurements. However, the present work provides deeper insight into the constraining of the diffusive dark fluid model by incorporating early-time measurements of the Cosmic Microwave Background (CMB) from the Planck 2018 data, together with recent late-time measurements of Baryon Acoustic Oscillation (BAO) data from the Dark Energy Spectroscopic Instrument (DESI) DR2 (2024). We employ the Monte Carlo Markov chain (MCMC) simulation using the modified `CLASS`[1] code [27] together with `COBAYA`[2] [28] for constraining the model parameters. We further analyze the scale-dependent behavior and the matter power spectrum to investigate the effects of the diffused dark fluid and to highlight its contribution to structure formation.

The paper is organized as follows: In Section 2, we review the basic equations for the background Universe, focusing on the diffusive dark-fluid system. The perturbation equations are presented in Section 3. The constraining of cosmological parameters from MCMC simulations is done in Section 4. In this section, the numerical results of the work are broadly explained. Finally, in Sec. 5, the conclusions are drawn up.

[1] `http://class-code.net/`

[2] `https://cobaya.readthedocs.io/en/latest/`

2 Basic equations

As presented in Refs. [24–26], the non-conservative energy-momentum tensor for the dark energy and dark matter components of the fluid is given by

$$\nabla_\mu T^{\mu\nu}_{de} = -\nabla_\mu T^{\mu\nu}_{dm} = N^\nu = \gamma_i u^\nu \ ,$$

where the current of the diffusion term for that fluid, $N^\nu_i = \gamma_i u^\nu$, γ_i represents the number density, and u^μ: $u^\nu u_\nu = -1$ is the four-velocity of the fluids. The 00-component of the interaction term reads $N^0 = \gamma_i u^0$, where $u^0 = \frac{1}{a}(1,0,0,0)$, $N^0 = \gamma_i/a^3$ for a homogeneous Universe, where the full detail is presented in [1, 29].

Projecting the above covariant conservation equations onto a homogeneous and isotropic FLRW background yields the continuity equations commonly employed in phenomenological interacting dark energy (IDE) models.In such models, the background conservation equations are commonly written as

$$\dot{\rho}_{\rm dm} + 3H\rho_{\rm dm} = Q_{\rm int}, \tag{1}$$
$$\dot{\rho}_{\rm de} + 3H(1+w_{\rm de})\rho_{\rm de} = -Q_{\rm int}, \tag{2}$$

thus guaranteeing total dark-sector energy conservation. With this convention, $Q_{\rm int} > 0$ corresponds to energy transfer from dark energy to dark matter, while $Q_{\rm int} < 0$ corresponds to energy transfer from dark matter to dark energy. In the diffusive model considered here, the interaction source for each component is $Q^{\rm i}_{\rm int} = \frac{\gamma_i}{a^3}$, with $\sum_i \gamma_i = 0$, so that $Q^{\rm dm}_{\rm int} = \gamma_{\rm dm}/a^3$ and $Q^{\rm de}_{\rm int} = \gamma_{\rm de}/a^3 = -Q^{\rm dm}_{\rm int}$. Identifying the interaction source as $Q^{\rm i}_{int} = \gamma_i/a^3$, the continuity equation for each fluid becomes: [29, 30]:

$$\dot{\rho}_i + 3\frac{\dot{a}}{a}(1+w_i)\rho_i = \frac{\gamma_i}{a^3} \ , \quad \text{where } i = b, dm, de. \tag{3}$$

Here $\gamma_{\rm b} = 0$ for baryons, while $\gamma_{\rm dm}$ and$\gamma_{\rm de}$ are constant diffusion parameters satisfying: $\gamma_{\rm dm} + \gamma_{\rm de} = 0$, which guarantees the conservation of the dark-sector energy. From Eq. 3, the conservation equation for each fluid becomes

$$\dot{\rho}_{de} + 3\frac{\dot{a}}{a}(1+w_{de})\rho_{de} = \frac{\gamma_{de}}{a^3} \ , \quad \dot{\rho}_{dm} + 3\frac{\dot{a}}{a}\rho_{dm} = \frac{\gamma_{dm}}{a^3} \ , \text{ and } \quad \dot{\rho}_b + 3\frac{\dot{a}}{a}\rho_b = 0 \ . \tag{4}$$

We assume the dark energy, where the pressure is taken $p_{de} = w_{de}\rho_{de}$, with equation-of-state parameter $w_{de} = -1$. A detailed mathematical expression is presented in Ref. [1]. The above diffusive solution of Eq. (4) leads to

$$H^2 = \frac{8\pi G}{3c^4}\left[\rho_{\rm m0}a^{-3} + \frac{\gamma_{\rm dm}}{H_0}\left(a-1\right)a^{-3} + \rho_{de0} - \frac{\gamma_{de}}{2H_0}\left(a^{-2}-1\right)\right] , \tag{5}$$

where $\rho_{m0} = \rho_{\rm b0} + \rho_{\rm dm0}$. The dimensionless dynamical quantities, see [1]:

$$\Omega_i \equiv \frac{8\pi G}{3H_0^2}\rho_i \ , Q_{dm} \equiv \frac{8\pi G}{3H_0^3}\gamma_{dm} = -Q_{de} \ , h \equiv \frac{H(z)}{H_0} \ .$$

We proceeded with further analysis using the above background evolution equations together with the following perturbation quantities presented in the following section.

3 Linear perturbations in diffusive cosmology

In the conformal-Newtonian gauge, the perturbed metric is

$$ds^2 = a^2(\tau)\Big[-(1+2\Phi)d\tau^2 + (1-2\Psi)\delta^{ij}dx_i dx_i\Big] \,, \tag{6}$$

where Φ and Ψ are the gravitational potentials. In the perturbed universe, the stress-energy-momentum tensor of the diffusive fluid is given as

$$\delta\left(T_i^{\mu\nu}{}_{;\mu}\right) = \delta N_i^{\nu} \,, \qquad \nabla_\mu \delta T_{de}^{\mu\nu} = -\nabla_\mu \delta T_{dm}^{\mu\nu} = \delta\left(N_i^{\mu}\right) \,, \tag{7}$$

where the diffusion term can be expressed $N_i^\mu = Q_{int}^\mu(i)u^\mu$, where the interacting diffusive term $N_i^\mu + \delta N_i^\mu \equiv \delta Q_{int}^\mu(i)u^\mu + Q_{int}^\mu(i)\delta u^\mu$, where $u^0 = \frac{1}{a}(1-\Phi)$ and $u^i = \partial_i v^i$ and the velocity $\theta_i = \partial_j v_i^j$. By taking into account Eq. (7), the perturbed quantities can be expressed: interaction term seems $\left(\delta Q_{int}^0(i) = -\frac{\gamma_i}{a}\Phi, \;\; \delta Q_{int}^i(i) = -\frac{\gamma_i}{a}v^i\right)$, and the four velocity vector $u^\mu = \tilde{u^\mu} + \delta u^\mu$, the pressure of the fluid $p_i = \tilde{p}_i + \delta p_i$, the density perturbation $\rho_i = \tilde{\rho}_i + \delta\rho_i$, for each species. The density perturbation at a comoving location x is most conveniently characterized by its fractional difference $\delta(x,t)$ with respect to the background Universe, $\delta_i(x,t) \equiv \frac{\rho_i - \tilde{\rho}_i}{\tilde{\rho}_i}$.

From Eq. (7), the 00 components of the energy momentum tensor is $\delta T_i^{00} = -\delta\rho_i$, the $0-i$ components $\delta T^{0j} = (\rho_i + pi)v_i^j$ and the ij components are $\delta T_i^j = \delta p_i \delta_i^j$. The generalized form of the density contrast and momentum conservation equations are [31, 32]

$$\begin{aligned}
&\delta_i' + 3\mathcal{H}(1+c_{si}^2)\delta_i - (1+w_i)(3\Phi' - \theta_i) + 9\mathcal{H}((1+w_i)(c_{s(i)}^2 - w_i)) = \frac{a}{\rho_i}\delta Q_{int}^0(i) \\
&+ \frac{aQ_{int}^0(i)}{\rho_i}\left[\Psi - \delta_i + 3\mathcal{H}(c_{s(i)}^2 - w_i)\frac{\theta_i}{\kappa^2}\right] \,, \;\; \text{and} \qquad (8) \\
&\theta_i' + \mathcal{H}(1-3w_i)\theta_i - k^2\Phi - \kappa^2\frac{c_{si}^2\delta_i}{(1+w_i)} = \frac{ak^2}{(1+w_i)\rho_i}\delta Q_{int}^j(i) + \frac{Q_{int}^0(i)}{\rho_i(1+w_i)}(\theta_i - (1+c_{si}^2)\theta_i) \,, \qquad (9)
\end{aligned}$$

respectively.

In the recent work [1], the effect of the density contrast of dark energy is highlighted as being neglected. This work emphasizes that the dominant role of matter perturbations in having a significant effect on gravitational collapse, which is the cause of structure formation, rather than that of dark energy, $\delta_{de} \approx 0$. This is because dark energy ($w = -1$) has no perturbations, and for canonical scalar-field dark energy $c_{si}^2 \approx 1$, pressure support smoothes out perturbations on subhorizon scales. In the current manuscript, we assume the coupling of the interaction term N_i^μ is purely timelike, and then $\delta N_i^j = 0$, so dark energy remains effectively homogeneous. We also assume that, for this fluid, we only consider the energy transfer and neglect the momentum transfer, where the energy transfer in the dark matter fluid affects the background and density contrasts more directly than the momentum transfer, see more in the Ref. [31]. We shall take into account Eqs. (8) and (9) for further discussion of the structure formation in diffusive dark fluid cosmology in the next section.

4 Results and Discussion

In this section, we have implemented the modified `CLASS` code [27] together with `COBAYA` [28] to constrain the diffusive dark fluid model for further analysis. To constrain the cosmological

parameters of the diffusive model, the following measurements are considered:

- **CMB:** From the *Planck* 2018 legacy release, we use the high-ℓ `Plik` TT likelihood ($30 \leq \ell \leq 2508$), TE and EE ($30 \leq \ell \leq 1996$), low-ℓ TT ($2 \leq \ell \leq 29$), low-ℓ EE ($2 \leq \ell \leq 29$), and the CMB lensing power spectrum [33]. We refer to this dataset as `Planck2018`.
- **BAO:** We use the DR2 BAO distance and correlation measurements from the Dark Energy Spectroscopic Instrument (DESI) [7, 34]. These include isotropic BAO measurements $D_V(z)/r_d$ and anisotropic measurements $D_M(z)/r_d$ and $D_H(z)/r_d$, as well as their correlations. Hereafter, we refer to this dataset as `DESI DR2 BAO`.
- **Joint datasets**: The combined analysis of the data improves the precision and constraints on the models we employ, providing a more complete picture of the Universe; for the joint analysis, we use `Planck2018`+`DESI DR2 BAO`, for which the corresponding chi-square is

$$\chi^2_{\text{sum}} = \chi^2_{\texttt{Planck2018}} + \chi^2_{\texttt{DESI DR2 BAO}} \,. \tag{10}$$

The contour plots of the constrained values of the considered cosmological parameters are presented in Fig. 1 using `Planck-2018` and `Planck-2018+DESI DR2 BAO` measurements by taking into account the parameter's priors as follows: H_0 [km/s/Mpc] $\in [0.5, 1.0]$; $\Omega_m \in [0.0, 1.0]$; $Q_{dm} \in [-0.1, 0.1]$; $n_s \in [0.8, 1.2]$; $\log A \in [1.61, 3.91]$; $\sigma_8 \in [0.0, 0.1]$; and $\theta_{s100} \in [0.5, 10]$. Similarly, Table 1 summarizes the 95% level of confidence of parameter values for ΛCDM and diffusive dark fluid models.

In the present work, we emphasize how intractable dark energy affects the evolution of the uni-

Parameters	**Diffusive model**		**ΛCDM** model	
	`Planck 2018`	`Planck 2018 + DESI DR2 BAO`	`Planck 2018`	`Planck 2018 DESI DR2 BA`
$\log(A_s)$	$3.044^{+0.016}_{-0.016}$	$3.047^{+0.013}_{-0.015}$	$3.046^{+0.017}_{-0.018}$	$3.047^{+0.015}_{-0.016}$
n_s	$0.9717^{+0.0037}_{-0.0036}$	$0.9715^{+0.0034}_{-0.0032}$	$0.9643^{+0.0047}_{-0.0038}$	$0.9707^{+0.0042}_{-0.0031}$
$Q_{\rm dm}$	$0.0005904^{+0.00034}_{-0.00034}$	$0.0005629^{+0.00033}_{-0.00034}$	—	—
H_0	$68.52^{+0.310}_{-0.310}$	$68.51^{+0.38}_{-0.41}$	$67.32^{+0.52}_{-0.51}$	$68.31^{+0.38}_{-0.33}$
Ω_m	$0.2996^{+0.0038}_{-0.0038}$	$0.2996^{+0.0035}_{-0.0041}$	$0.3154^{+0.0075}_{-0.0071}$	$0.3022^{+0.0038}_{-0.0042}$
σ_8	$0.8105^{+0.006}_{-0.0064}$	$0.8113^{+0.0059}_{-0.006}$	$0.811^{+0.0079}_{-0.0075}$	$0.806^{+0.0063}_{-0.0056}$
Statistical values				
χ^2	2775.85	2791.88	2776.25	2793.33
AIC/ΔAIC	2789.85/1.599	2805.88/0.080	2788.25/—	2805.33/—
BIC/ΔBIC	2830.62/7.420	2846.69/5.980	2823.20/—	2840.31/—

Table 1: The table shows the parameter values for ΛCDM and diffusive dark fluid models at 68% level of confidence and the statistical values of the models.

verse through a diffusion mechanism. The parameter Q_{dm} is the key quantity that indicates the flow of energy in the system. As presented in Table 1, the values of $Q_{\rm dm}$ are $0.0005904^{+0.00034}_{-0.00034}$ and $0.0005629^{+0.00033}_{-0.00034}$ for the `Planck 2018` and `Planck 2018 + DESI DR2 BAO` datasets respectively. The sign of Q_{dm} indicates the direction of the energy flow, as presented in [1]. For

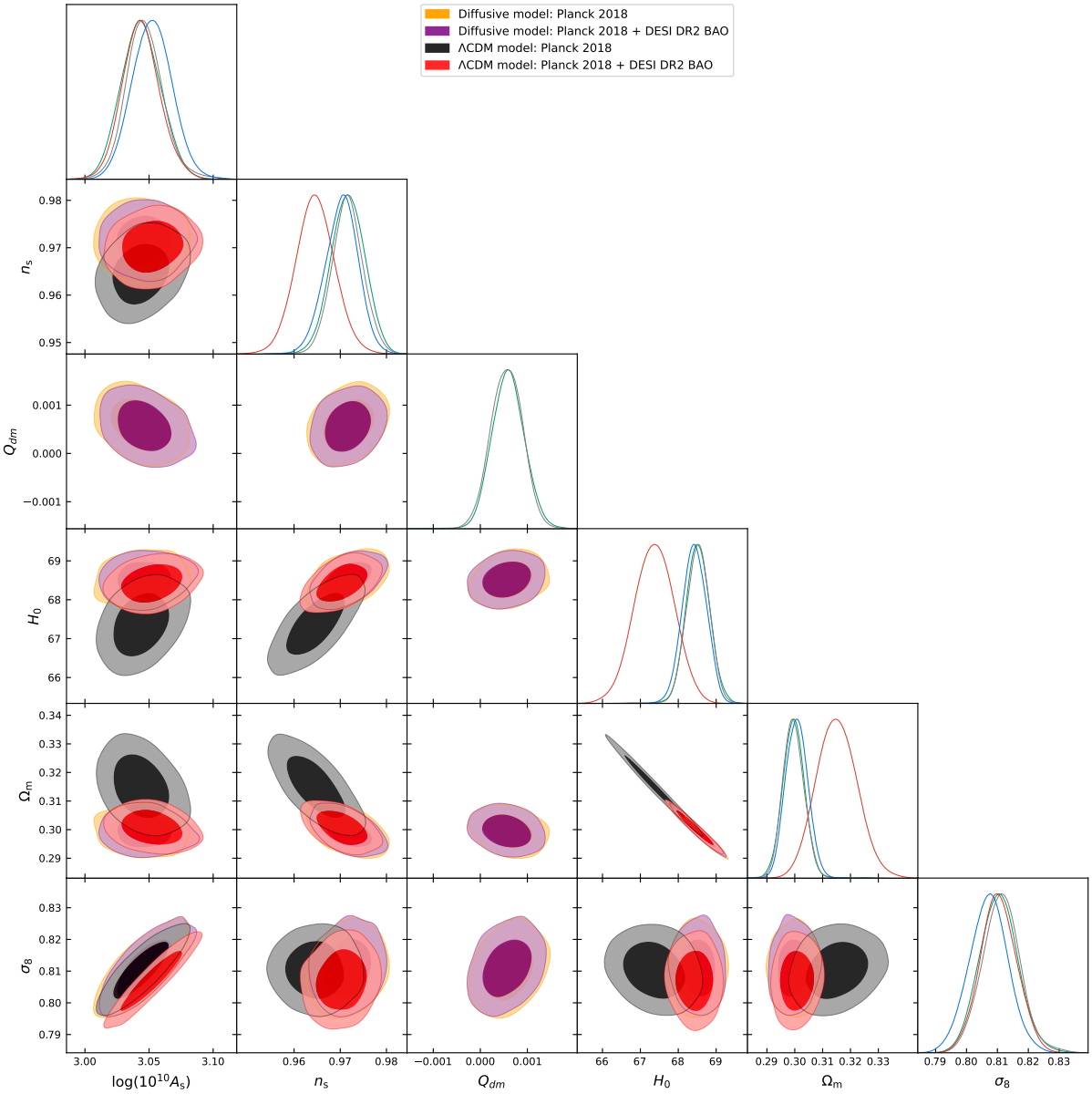


Figure 1: The MCMC output for diffusive and ΛCDM models at 68% level of confidence space for the posterior parameters for `Planck-2018` and `Planck-2018+DESI DR2 BAO` measurements

instance, when $Q_{dm} < 0$, the flow of energy is from dark matter to dark energy, and the opposite conclusion is true. Based on the results presented in Table 1, these are the best-fit values of $Q_{dm} > 0$, indicating the flow of energy is from dark energy to dark matter for the considered measurements. This result is also consistent with the recent finding [35, 36].

From this table, we note that the deviation between our diffusive model values of $H_0 = 68.52^{+0.310}_{-0.310}$ and $68.51^{+0.38}_{-0.41}$ and the Planck 2018 result $H_0 = 67.4 \pm 0.5$ km/s/Mpc [33] is 1.90σ and 1.72σ, respectively. For the ΛCDM model, $H_0 = 67.32^{+0.52}_{-0.51}$, & $68.31^{+0.38}_{-0.33}$ corresponds to 0.120σ and 1.519σ. Similarly, the sigma deviations of the H_0 values taken from the Table 1 and the SH0ES measurement $H_0 = 73.04 \pm 1.04$ [37] are 4.17σ and 4.09σ for the diffusive model, and 4.91σ and 4.27σ for the ΛCDM model. Indeed, the deviation between the SNIa (SH0ES) and Planck 2018 measurements of H_0 is 5.28σ. Using the same models, the sigma deviation is presented

[1] and reported that the diffusive model is favored by Planck 2018 measurements, while the ΛCDM model is favored by SH0ES measurements. In the current study, both models are statistically consistent with Planck 2018 measurements but show strong tension with SH0ES, with deviations $\geq .27\sigma$. A full analysis will be considered in upcoming work with more extensive data sets, including `Planck 2018 + SNIa` compilations.

In this work we also highlight the statistical analysis of the diffusive model by calculating the minimum Chi-squre (χ^2_{min}) Akaike Information Criterion ($\mathrm{AIC} = \chi^2_{\mathrm{min}} + 2\mathrm{K}$) and the Bayesian/Schwarz Information Criterion ($\mathrm{BIC} = \chi^2_{\mathrm{min}} + \mathrm{K}\log(\mathrm{N_i})$), where K corresponds to the number of free parameters for that specific model, and N_i stands for the number of data points for the i^{th} dataset, see Table 1. From Table 1, the values of $\Delta\mathrm{AIC} \leq 2$, indicate that the model has substantial support for the observational evidence.[3] For more information see Ref. [38]. Whereas $\Delta\mathrm{BIC}$ value found in the range of $6 \leq \Delta\mathrm{BIC} \leq 10$, which indicates the model has weak observational support. However, this statistical penalization comes from the large number of data points and the model's extra degree of freedom, not the physical viability of the considered model. Beyond information criteria, discrimination within the interacting dark-energy class can be sharpened by demanding simultaneous consistency at the background (H_0), growth-amplitude (σ_8) and perturbation-coupling levels. This view, that cosmological tensions act as consistency conditions on a given model, has been formalised as the cosmological consistency triangle [39] and applied to modified-gravity deviations [40].

By accounting for the constraint values for the cosmological parameters taken from Table 1, we present numerical results for the scale-dependent density contrast $|\delta|_m(z,\kappa)$ and the matter power spectrum $P_m(k,z)$ for the diffusive dark-fluid model and compare them with ΛCDM. First, we show numerical results for the scale-dependent density contrast $|\delta|_m(z,k)$ (see Fig.2) for the diffusive dark-fluid model with wave-mode scale $k = 0.0001\ \mathrm{Mpc}^{-1}$. The scale-independent density contrast for the same model is discussed in [1], where $|\delta|_m(z,k) = |\delta|_m(z)$. In this plot, we clearly see that the diffusive dark-energy model exhibits small deviations from ΛCDM near $z \approx 0$, indicating that energy transfer via diffusion affects late-time cosmic evolution.

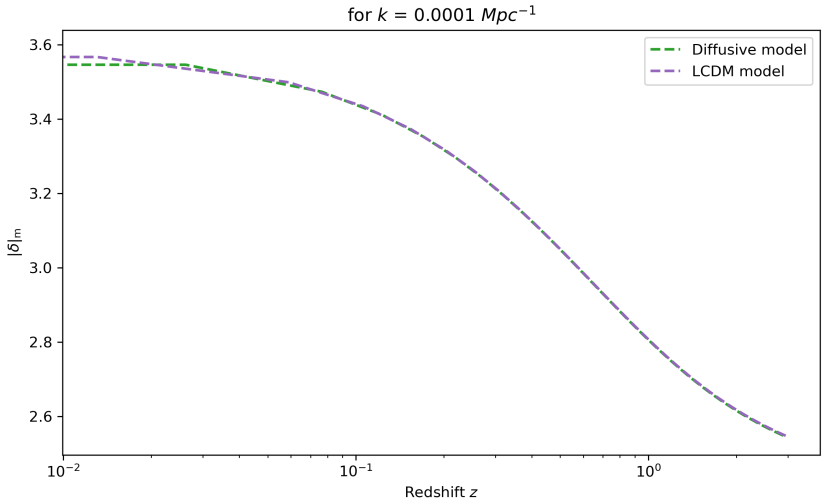


Figure 2: The scale-dependent density contrast $|\delta|_m(z,k)$ for diffusive dark fluid and ΛCDM models.

[3] $\Delta\mathrm{AIC} = \Delta\mathrm{AIC}_{\mathrm{diffusive}} - \Delta\mathrm{AIC}_{\Lambda\mathrm{CDM}}$

We secondly present the numerical results of the matter power spectrum $P_m(k,\ z=0,1)$ at redshifts $z=0$ and 1 at left panel of Fig 3. From this plot, the amplitude of the power spectrum is generally higher than that of the diffusive fluid model due to the energy transfer through diffusion interaction. This deviation of the power spectrum $\Delta P_m(k,\ z=0,1)$ is more clearly noticeable in Fig 3, where the deviation is

$$\Delta P_m(k,\ z=0,1) = \frac{P_m^{\rm diffusive}(k,\ z=0,1) - P_m^{\Lambda{\rm CDM}}(k,\ z=0,1)}{P_m^{\Lambda{\rm CDM}}(k,\ z=0,1)}\ .$$

From the numerical results of $\Delta P_m(k,\ z=0,1)$ in the right panel of Fig. 3, we observe that the effect of the interaction for the matter fluctuations across different k ranges. At least the following three cases are noticeable:

- For the case of small scale $k \gtrsim 10^{-1} h\,{\rm Mpc}^{-1}$, we observe that oscillation curves of the matter spectrum, $\Delta P_m(k,\ z=0,1)$ due to BAO-like wiggles), where the diffusive model enhance of the matter fluctuations than ΛCDM were more clustering in this scale.

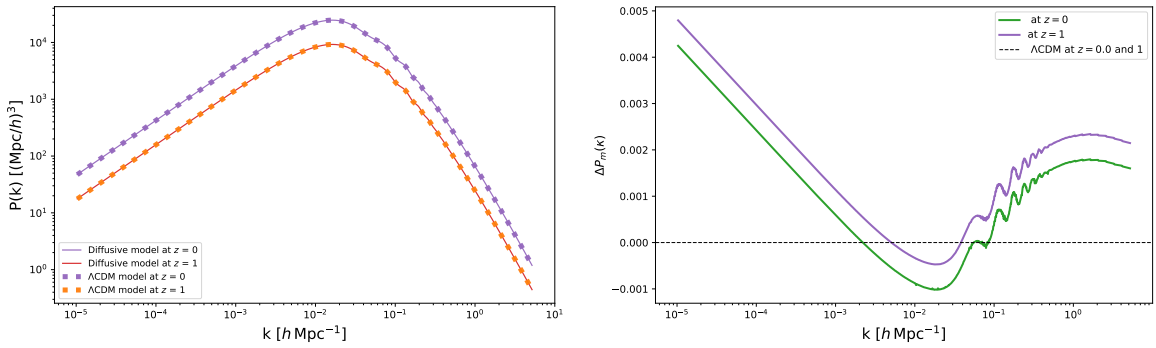


Figure 3: Left panel: the matter power spectrum $P_m(k,\ z=0,1)$ for diffusive dark fluid and ΛCDM models. Right panel: the deviation of matter power spectrum $\Delta P_m(k,\ z=0,1)$ between diffusive dark fluid and ΛCDM models.

- For the case of intermediate scale around $10^{-2} \lesssim k \lesssim 10^{-1} h\,{\rm Mpc}^{-1}$, we clearly see the monotonically suppressed matter fluctuation against ΛCDM.
- For the case of large scale $k \lesssim 10^{-2} h\,{\rm Mpc}^{-1}$, the deviation of the power spectrum $\Delta P_m(k,\ z=0,1)$ is nearly smooth and monotonically increased the amplitude of the $\Delta P_m(k,\ z=0,1)$, where the diffusive model enhancing the matter fluctuations at this range as well. In general, the amplitude of the $P_m(k)$ at $z=1$ is higher than at $z=0$ across all scales.

5 Conclusions

In this manuscript, we revised the interacting dark energy through a diffusion mechanism with the `Planck-2018` and `DESI BAO DR2` measurements. After we highlighted the basic equations of the conservation equation, we demonstrate that the MCMC simulation can constrain the cosmological parameters using the modified `CLASS` code together with `COBAYA`. We have

highlighted the H_0 tension based on the Hubble parameter values taken from Table 1 and reported that the diffusive model has a statistical consistency with Planck 2018 but strong tensions with SH0ES.

The best-fit values of $Q_{\rm dm}$ are positive, whereas Ref. [1] reported negative values using late-time background and growth data. Under the common sign convention adopted in both analyses, $Q_{\rm dm} < 0$ corresponds to energy transfer from dark matter to dark energy, while $Q_{\rm dm} > 0$ corresponds to transfer from dark energy to dark matter. However, the credible intervals obtained here include $Q_{\rm dm} = 0$, so the apparent difference in the best-fit sign should not be interpreted as evidence for a statistically established reversal of the energy-transfer direction. It may instead reflect differences in the datasets, parameter degeneracies, or the treatment of the background and perturbation sectors. Including the combinations of early- and late-time measurements makes the results more reliable than work done using only late-time measurements.

The detailed statistical analysis of the model is highlighted by calculating the $\chi^2_{\rm min}$, ΔAIC, ΔBIC to test the good fit of the model with the observations. From the results, the model has been strongly supported according to ΔAIC, but weaker support from the ΔBIC point of view. The work also emphasized the numerical results of the scale-dependent density contrast and the matter power spectrum. We also present the deviation of the power-spectrum $\Delta P_m(k,\ z = 0, 1)$ that clearly showed the significant effects of the diffusive interaction against ΛCDM. In the upcoming work, the comprehensive analysis with intensive datasets will be conducted to see the overall picture of the diffusive dark fluid model that possibly alleviates the cosmological tensions.

References

[1] Shambel Sahlu et al. Observational constraints of diffusive dark-fluid cosmology. *Monthly Notices of the Royal Astronomical Society*, 546(1):staf1921, 2026.

[2] Adam G Riess et al. Observational evidence from supernovae for an accelerating universe and a cosmological constant. *The Astronomical Journal*, 116(3):1009, 1998.

[3] Saul Perlmutter et al. Measurements of Ω and Λ from 42 high-redshift supernovae. *The Astrophysical Journal*, 517(2):565, 1999.

[4] Philip Bull et al. Beyond ΛCDM: Problems, solutions, and the road ahead. *Physics of the Dark Universe*, 12:56–99, 2016.

[5] N Aghanim et al. Planck 2018 results. VI. Cosmological parameters. *Astron. Astrophys*, 641:A6, 2020.

[6] Thibaut Louis et al. The Atacama Cosmology Telescope: DR6 power spectra, likelihoods and ΛCDM parameters. *Journal of Cosmology and Astroparticle Physics*, 2025(11):062, 2025.

[7] M Abdul Karim et al. DESI DR2 results. II. Measurements of baryon acoustic oscillations and cosmological constraints. *Physical Review D*, 112(8):083515, 2025.

[8] David N Spergel et al. First-year Wilkinson Microwave Anisotropy Probe (WMAP)* observations: determination of cosmological parameters. *The Astrophysical Journal Supplement Series*, 148(1):175, 2003.

[9] Steven Weinberg. The cosmological constant problem. *Reviews of modern physics*, 61(1):1, 1989.

[10] David N Spergel. The dark side of cosmology: Dark matter and dark energy. *Science*, 347(6226):1100–1102, 2015.

[11] Eleonora Di Valentino et al. Interacting dark energy in a closed universe. *Monthly Notices of the Royal Astronomical Society: Letters*, 502(1):L23–L28, 2021.

[12] Li-Yang Gao et al. Relieving the H_0 tension with a new interacting dark energy model. *Journal of Cosmology and Astroparticle Physics*, 2021(07):005, 2021.

[13] Marcel van der Westhuizen et al. Compartmentalization in the dark sector of the universe after DESI DR2 BAO data. *Physics of the Dark Universe*, page 102107, 2025.

[14] Shambel Sahlu et al. Testing the coexistence of dark energy and dark matter with late-time observational data. *Physics of the Dark Universe*, page 102280, 2026.

[15] Bo-Yu Pu, Xiao-Dong Xu, Bin Wang, and Elcio Abdalla. Early dark energy and its interaction with dark matter. *Physical Review D*, 92(12):123537, 2015.

[16] Riccardo Murgia, Stefano Gariazzo, and Nicolao Fornengo. Constraints on the coupling between dark energy and dark matter from CMB data. *Journal of Cosmology and Astroparticle Physics*, 2016(04):014, 2016.

[17] Yuejia Zhai et al. A consistent view of interacting dark energy from multiple CMB probes. *Journal of Cosmology and Astroparticle Physics*, 2023(07):032, 2023.

[18] Caldera-Cabral et al. The growth of structure in interacting dark energy models. *Journal of Cosmology and Astroparticle Physics*, 2009(07):027, 2009.

[19] Jian-Hua He, Bin Wang, and YP Jing. Effects of dark sectors' mutual interaction on the growth of structures. *Journal of Cosmology and Astroparticle Physics*, 2009(07):030, 2009.

[20] Yun Liu et al. Dark matter haloes in interacting dark energy models: formation history, density profile, spin, and shape. *Monthly Notices of the Royal Astronomical Society*, 511(2):3076–3088, 2022.

[21] M Hashim et al. Cosmic degeneracies III: N-body simulations of interacting dark energy with non-Gaussian initial conditions. *Monthly Notices of the Royal Astronomical Society*, 481(3):2933–2945, 2018.

[22] Bin Wang et al. Dark matter and dark energy interactions: theoretical challenges, cosmological implications and observational signatures. *Reports on Progress in Physics*, 79(9):096901, 2016.

[23] Matteo Lucca. Multi-interacting dark energy and its cosmological implications. *Physical Review D*, 104(8):083510, 2021.

[24] Zbigniew Haba. Energy and entropy of relativistic diffusing particles. *Modern Physics Letters A*, 25(31):2683–2695, 2010.

[25] Simone Calogero. A kinetic theory of diffusion in general relativity with cosmological scalar field. *Journal of Cosmology and Astroparticle Physics*, 2011(11):016, 2011.

[26] David Benisty et al. Unification of dark energy and dark matter from diffusive cosmology. *Physical Review D*, 99(12):123521, 2019.

[27] Diego Blas, Julien Lesgourgues, and Thomas Tram. The cosmic linear anisotropy solving system (CLASS). Part II: Approximation schemes. *Journal of Cosmology and Astroparticle Physics*, 2011(07):034, 2011.

[28] Jesus Torrado and Antony Lewis. Cobaya: Code for bayesian analysis of hierarchical physical models. *Journal of Cosmology and Astroparticle Physics*, 2021(05):057, 2021.

[29] Zbigniew Haba et al. Dynamics of the diffusive dm-de interaction–dynamical system approach. *Journal of Cosmology and Astroparticle Physics*, 2016(07):024, 2016.

[30] Subhayan Maity et al. Universe consisting of diffusive dark fluids: thermodynamics and stability analysis. *The European Physical Journal C*, 79:1–8, 2019.

[31] Jussi Väliviita et al. Large-scale instability in interacting dark energy and dark matter fluids. *Journal of Cosmology and Astroparticle Physics*, 2008(07):020, 2008.

[32] Elisabetta Majerotto et al. Adiabatic initial conditions for perturbations in interacting dark energy models. *Monthly Notices of the Royal Astronomical Society*, 402(4):2344–2354, 2010.

[33] Nabila Aghanim et al. Planck 2018 results-VI. Cosmological parameters. *Astronomy & Astrophysics*, 641:A6, 2020.

[34] Uendert Andrade et al. Validation of the DESI DR2 measurements of baryon acoustic oscillations from galaxies and quasars. *Physical Review D*, 112(8):083512, 2025.

[35] Anderson Almeida Escobal et al. Linear growth of matter perturbations probed by redshift-space distortions in interacting $\Lambda(t)$ CDM cosmologies. *Physics of the Dark Universe*, page 102320, 2026.

[36] David Figueruelo, Marcel van der Westhuizen, Amare Abebe, and Eleonora Di Valentino. Late-time background constraints on linear and non-linear interacting dark energy after DESI DR2. *Physics of the Dark Universe*, 52:102238, 2026.

[37] Adam G Riess et al. Large Magellanic Cloud Cepheid standards provide a 1% foundation for the determination of the Hubble constant and stronger evidence for physics beyond ΛCDM. *The Astrophysical Journal*, 876(1):85, 2019.

[38] Shambel Sahlu, Álvaro de la Cruz-Dombriz, and Amare Abebe. Structure growth in $f(Q)$ cosmology. *Mon. Not. Roy. Astron. Soc.*, 539(2):690–703, 2025.

[39] Amare Abebe. The cosmological consistency triangle as a model-discrimination framework. *Preprints 202606.1423*, 2026.

[40] Amare Abebe. Cosmological tensions as consistency conditions for $f(Q)$ gravity. *arXiv preprint arXiv:2604.27773*, 2026. Contribution to the Corfu Summer Institute 2025, "Tensions in Cosmology" Workshop.